Analysis of the Convectively Modified GATE Boundary Layer Using *in situ* and Acoustic Sounder Data

J. E. GAYNOR

Wave Propagation Laboratory, Environmental Research Laboratories, NOAA, Boulder, CO 80302

C. F. ROPELEWSKI

Center for Environmental Assessment Services, Environmental Data Information Services, NOAA, Washington, DC 20235

(Manuscript received 2 January 1979, in final form 16 April 1979)

ABSTRACT

A boundary-layer categorization scheme based on GATE acoustic sounder data stratifies surface data and tethered balloon data from the NOAA research ship *Oceanographer*. The results indicate a clear increase in the sensible heat flux across the sea surface during disturbed conditions (the gravity current and storm wake of the disturbance) but no conclusive differences of latent heat and momentum fluxes. The tethered balloon profiles show a near disappearance of the mixed layer within the gravity current and, in the storm wake, a very shallow and cool mixed layer capped by a strong stable layer relative to the undisturbed category.

We calculate the vertical motion due to buoyancy-driven entrainment for a range of entrainment parameters after exploiting the categorized tethered balloon profiles to obtain mean gradients at the top of the mixed layer. Because we and others have observed that the shallow mixed-layer depth remains nearly constant with time in the storm wake, this calculated entrainment-induced vertical motion is balanced with an hypothesized mesoscale subsidence beneath the anvil in the wake. Even though our entrainment calculation ignores the possibly important but unknown effects of vertically propagating waves, breaking waves and wind shear, the integrated divergence derived from this subsidence agrees well with the range of mesoscale divergences in the storm wake presented by Zipser (1977).

1. Introduction

Prior to the GARP Atlantic Tropical Experiment (GATE) in the summer of 1974, detailed analysis of low-level atmospheric data in the tropical ocean regions, especially data from aircraft, indicated that precipitating convection had a profound effect on the tropical marine boundary layer. A review article by Garstang and Betts (1974), the measurements of sea surface fluxes of Aspliden (1976) and the modeling work of Johnson (1976) all pointed to similar conclusions. Downdrafts within and in the vicinity of precipitating convection reach very close to the ocean surface, effectively replacing the mixed layer during and immediately following the precipitation and leading to a surprisingly long duration of significant large-scale low-level stabilization.

The analysis of boundary layer (defined here as the mixed layer and lower cloud layer encompassing the fair weather cumuli) measurements from GATE now coming to light essentially confirm the conclusions based on the pre-GATE data sets. The GATE boundary layer data have allowed computation of flux profiles within the convectively modified regions and have allowed comparison of these profiles with those in undisturbed situations (e.g., Wylie, 1976; Emmitt, 1978). The recent efforts of Zipser (1977) and Houze (1977) have combined radar, surface, tethered sonde and radiosonde profiles, and aircraft and acoustic sounder data in an attempt to look at the total picture of precipitating convection in GATE. Not only did they study the evolution of individual convective elements within a mesoscale structure, but they also looked at some of the effects of this convection on the entire troposphere, including the boundary layer. Their analysis helps to explain the formation of the long-lasting, strong, stable layer, now often called the "wake" region, following the precipitation.

The atmospheric acoustic sounder which was deployed on the NOAA ship *Oceanographer* during the three phases of GATE also gives an excellent picture of the modified boundary layer, including the wake region. The acoustic sounder records, in conjunction with high-resolution tethered sonde profiles and surface data, provide a detailed description of the convectively modified boundary layer during GATE.

The work reported on here focuses on the boundary layer modified by precipitating convection during GATE and uses the acoustic sounder facsimile data as an indicator of the density current (often called "gust front") arrival and of the eventual breakup of the wake regime. The next section will distinguish between density current and wake regions. We prefer to use the term "density current" rather than "gust front" because the mean data will not always show a distinct wind gust even at the time of the arrival of the current. The usage agrees with that of Charba (1972) and Hall *et al.* (1976).

Using a classification scheme based on the appearance of the acoustic facsimile data, we divide the boundary layer into three categories: undisturbed, early perturbed (density current) and mature perturbed (wake). Temporal and first-order statistics using data from the *Oceanographer* Surface Meteorological Sensing System (SMSS), along with sounder data, will indicate the longevity and thermodynamical effects of the disturbances on the boundary layer. Categorized bulk-flux data from the ocean's surface, integrated with similarly composited tethered-balloon profile data, allow a discussion of the observed boundary-layer dynamics in disturbed as well as undisturbed situations. We compare the observations presented here with those of Houze (1977) and Zipser (1977), who have studied the detailed structure of tropical convection (in particular, the upper levels of the troposphere) in an attempt to tie in the boundary-layer processes with events in the upper atmospheric levels. We use a simple entrainment model to estimate the vertical transport balance required to maintain the inversion in the wake at a relatively constant low level.

2. Instrumentation

a. The acoustic sounder

An acoustic sounder mounted on the *Oceanographer* during the entire observation period (June–September 1974) of GATE provided an almost continuous record of the boundary-layer structure to a height of 850 m during both disturbed and undisturbed conditions. The earlier work of Mandics *et al.* (1975) and Mandics and Hall (1976) concerns the appearance of acoustic fascimile records during disturbed events. Gaynor and Mandics (1978) and Gaynor (1978) detail these boundary layer modifications using both acoustic sounder data and *in situ* data for comparison. Mandics and Owens (1975) explain the operation of the sounder.

The papers cited above present many examples of acoustic facsimile records for various boundary-layer conditions with fairly detailed explanations and interpretations. A facsimile record represents a time/height cross section of backscattered acoustic intensity from the atmosphere. Fig. 1, taken from a vertical pulsing-and-receiving acoustic sounder on

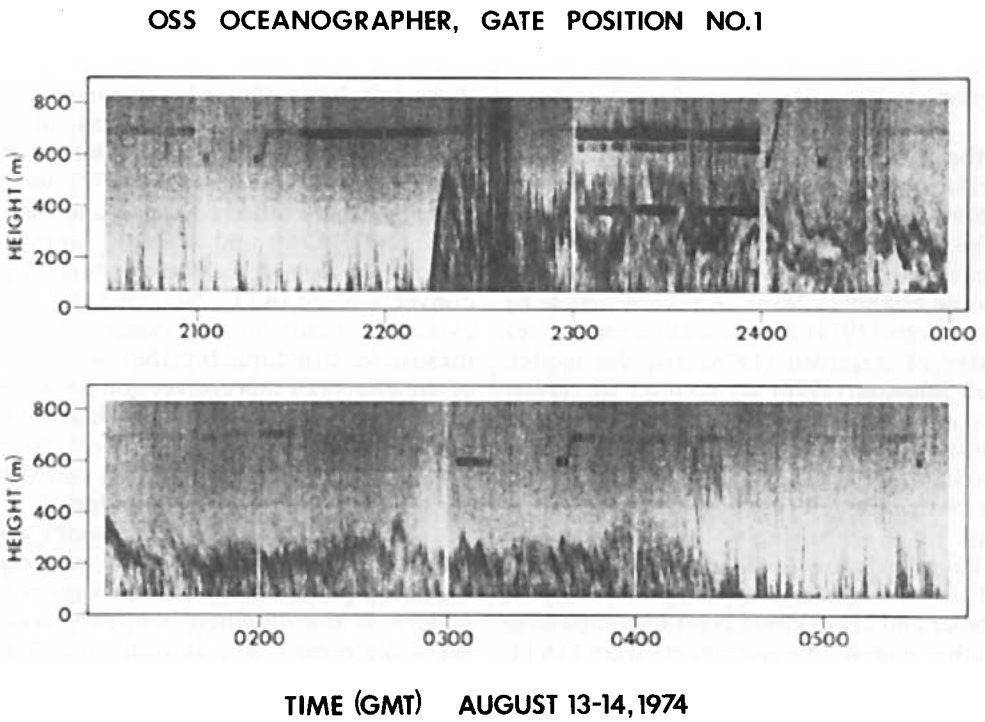

FIG. 1. An example of an acoustic facsimile record of the passage of a disturbance in the boundary layer caused by precipitating convection during GATE.

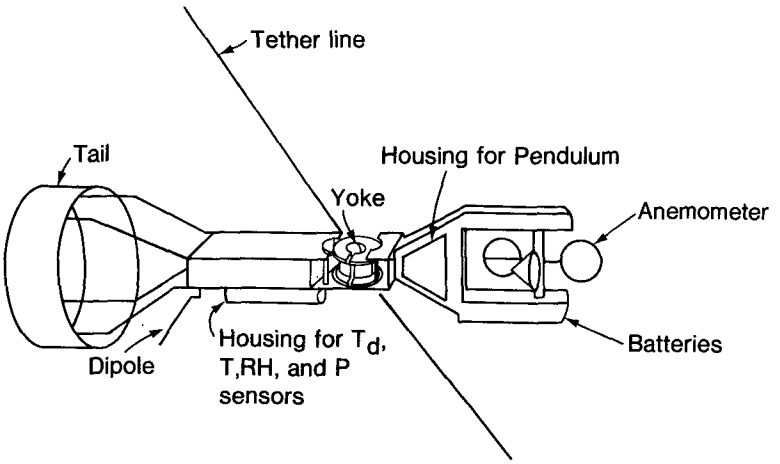

FIG. 2. The tethered sonde used in the BLIS.

the *Oceanographer*, presents an example of a facsimile record. The sound scatters from small-scale (~0.1 m) temperature and moisture fluctuations (Wesely, 1976), which often occur within layers of stability or within warm and moist thermal plumes rising from the relatively warm ocean surface. Within a stable layer or an inversion layer, wind shear enhances turbulence, which continually creates and destroys temperature and moisture gradients at the microscale and therefore enhances acoustic backscatter from that layer (Brown and Hall, 1978). These characteristics of the instrument response allowed measurement of the mixed-layer inversion height during the periods of a convectively modified boundary layer.

b. The tethered sonde

The Boundary Layer Instrument System (BLIS) provided high-resolution profiles from the surface to 1 km. BLIS consists of a tethered balloon, with as many as five sondes attached to the line at one time, and associated telemetry and recording systems. Each sonde (Fig. 2) measured wind speed and direction with a sampling rate of 0.5 Hz, and dry-bulb temperature, wet-bulb temperature, relative humidity and pressure with a sampling rate of 0.25 Hz. The ascent/descent rates during profiles varied between 1.0 and 2.5 m s^{-1}. The sondes often flew at fixed levels for several hours. The synoptic situation (i.e., more profiles during convectively active periods) and operational constraints (e.g., proximity of aircraft) determined the frequency of the profiles.

Burns (1974) describes the instrument and its design specification in detail and Ropelewski (1976) presents an error analysis of the GATE BLIS data. The 1 mb resolution profile data used in this study are part of the Convection Subprogram Data Center's Composite Data Set and are provided through the GATE *Data Catalogue* (EDS, 1975).

c. Surface data

Instruments mounted on a 10 m boom that extended from the bow of the *Oceanographer* measured shipboard winds and temperatures used in this study. The instrument's height above the sea surface was 10 m. Aspirated thermistors measured the wet- and dry-bulb temperatures and a Gill three-cup anemometer recorded the wind speed. A thermistor kept at a nominal depth of 10 cm measured the sea surface temperature. Seguin *et al.* (1977) report the details of the sensor characteristics. Computations of the fluxes and mean quantities use data initially recorded at 0.5 Hz and averaged at 3 min intervals.

3. Boundary-layer classification

The brief explanation of acoustic scattering in Section 2 permits an interpretation of the acoustic facsimile exemplified in Fig. 1. Until about 2215 GMT[1] on 13 August 1974, echoes from thermal plumes predominate. These are the dark, narrow, vertically oriented echoes rising from the bottom of the record. At 2215, a density current associated with precipitating convection passed over the ship accompanied by a drop in dry-bulb temperature near the surface and gusty surface winds. Very little rain occurred over the ship during this event although some rain noise is evident in the form of dark vertical lines from top to bottom of the record in Fig. 1 around 2230. Plume echoes have disappeared from 2215 to almost 2300, but just before 2300 they reappear. Gaynor and Mandics (1978) have shown that undulating echoes above the plumes from around 2300 until almost 0430 on the following day represent stable layers of strong wind shear. In fact, Readings *et al.* (1973) have shown that the protrusion of plumes into the stable layer

[1] All times GMT.

TABLE 1. Selected statistics from the disturbed boundary layer.

Parameter	Phase I	Phase II	Phase III	Total or average
Number of disturbances	49	39	49	137
Duration (h)				
Average	2.36	2.97	3.37	2.89
Maximum	16.45	13.45	16.68	
Percent of time in disturbed conditions	32	27	34	31
Dry-bulb temperature drop (°C)				
Average	1.27	1.10	1.43	1.28
Maximum	4.81	5.62	6.06	

enhances the wind shear and, therefore, will enhance the acoustic scatter. Intermittent acoustic reflections from the tethered balloon and its sondes cause the very dark, thick horizontal echoes at around 700 and 400 m. Background noise enhancement, which is due to an electronic adjustment of reception sensitivity to compensate for acoustic beam widening, causes the generally darker regions at the top of the record, especially noticeable prior to 2215.

The event between 2215 and 0430 exemplifies a disturbed boundary layer, modified by cool-air downdrafts beneath precipitating convection. We will delineate and composite similar events according to the following classification scheme based on the acoustic facsimile records:

1) Undisturbed: periods of thermal plumes, 2 h from any disturbance, within which we average *in situ* data.

2) Early perturbed or density current: in-situ data averaged 1 h or less after the start of the perturbation.

3) Mature perturbed or wake: *in-situ* data averaged between 4 h after the start of the perturbation and its ending.

Categories 2 and 3 attempt to separate the density current from the wake regimes, which, according to Zipser (1977), represent much different boundary layer dynamics in squall lines. (Zipser calls the density current the "squall front.") Category 1 avoids periods immediately after wake events when the mixed layer may not have totally recovered, and periods immediately before disturbances when mixed layer modification may occur.

In Fig. 1 the plume echoes before 2200 exemplify category 1, although in practice category 1 would have ended at about 2015, 2 h before the density current arrival. The time between 2215 and 2315 exemplifies category 2, and that from 0315 to almost 0430, category 3.

We chose the categories because the boundary layer looked very similar within each category in terms of its turbulence structure as seen on the acoustic facsimile records. The time separation between categories minimized contamination caused by the transition from one category to another. Clearly, this method of stratifying the data combines the strong squall lines with the very weak isolated cumulonimbus (even those which may not propagate directly over the ship) in category 2. Category 3 includes only the stronger events because the 4 h delay is longer than the average duration of a disturbed boundary layer (Table 1). We make the important (and perhaps naive) assumption that because the signature of turbulence appears similar within each category, the basic boundary layer dynamics within each category are also similar, regardless of the relative strengths of individual events making up a category. *A priori*, we have no reason to believe differently.

To supplement the acoustic records, visual inspection of the *Oceanographer* SMSS 10 m level dry-bulb temperature provided a very good indicator of the onset of category 2 and the duration of categories 2 and 3. Scientists on the ships from the Federal Republic of Germany also used bow-boom temperature depressions as indicators of a disturbed boundary layer (Hasse, personal communication). In virtually all cases in which both the temperature and acoustic data were simultaneously available, temperature decreases agreed with the typical disturbed boundary layer structure seen on the facsimile records (Fig. 1). After developing some skill in identifying the disturbances, we were able to confidently complete the statistics when only one set of data was available. However, the stable-layer signature of the acoustic records indicating category 3 generally persisted for a longer time than the temperature depression (Gaynor and Mandics, 1978).

Table 1 presents statistics of the disturbed boundary layer combining categories 2 and 3 at the *Oceanographer* positions. A total of 137 disturbances had an average duration of nearly 3 h, but with maxima over 16 h. These long-lasting events indicated organized squall lines of the type studied by Houze (1977). Six occurred in GATE, with three of them in Phase III. The boundary layer appeared disturbed 31% of the time during GATE according to the acoustic sounder classifications. Using an objective classification of tethered sonde profile data, Jalickee and Ropelewski (1979) have shown that about 30% of the temperature profiles indicate either a gravity current (category 2) or a wake (category 3) event (see Fig. 3). Also, D. Fitzjarrald (personal communication) at the University of Virginia has classified GATE radar data according to convective activity and has found that combining periods in which most of the region is covered with precipitation (comparable to our category 2)

with periods of no echo after the passage of organized convection (comparable to category 3) accounts for around 30% of the time. If these results mean that, on the average, convection modified about 30% of the GATE C-array boundary layer, this would have very important repercussions to boundary-layer energetics and modeling. The enhanced stabilities in the modified, shallow mixed layer during gravity current and wake events alters vertical transports through the top of the mixed layer. The average temperature drop from the bow-boom data during the passage of the density current was 1.3°C, but the largest drop, over 6°C, occurred at the arrival of the squall lines (squall front).

4. Analysis

a. Surface fluxes

The following expressions estimate the bulk aerodynamic fluxes from the sea surface at the *Oceanographer* (Gaynor and Mandics, 1978):

$$H = 1.53\ U_b(T_s - T_b)$$

$$LE = 3.74 \times 10^3\ U_b(q_s - q_b)$$

$$\tau = 1.53 \times 10^{-3}\ U_b^2.$$

Here the symbols are defined as

H sensible heat flux (W m^{-2})
LE latent heat flux (W m^{-2})
τ surface stress (N m^{-2})
U_b wind speed
T temperature
q specific humidity

and the subscripts (s,b) refer to sea surface and boom-level measurements, respectively. We assumed that the sea surface drag coefficient is the same for H, LE and τ (1.3×10^{-3}).

Table 2 shows the fluxes stratified by the scheme presented in the last section and normalized by the mean for each phase. The parentheses indicate the number of 3 min fluxes that went into each category. As stated above, the features appearing on the acoustic facsimiles look the same for either case, but are more persistent in the organized disturbances. The temperature drop at the 10 m level is another common feature. However, relatively strong surface winds do not necessarily predominate in the density current as the means of τ in Table 2 indicate.

TABLE 2. Ratio of the surface fluxes in each category to the mean.

	Category	Phase I		Phase II		Phase III	
Stress ($\tau/\bar{\tau}$)	1	0.8	(3066)	1.1	(1373)	1.1	(3409)
	2	1.7	(708)	1.1	(907)	1.0	(1034)
	3	1.1	(555)	0.6	(520)	0.6	(1281)
$\bar{\tau}$ (N m^{-2})		0.029	(4329)	0.043	(2800)	0.050	(5724)
Latent heat ($LE/\overline{LE}$)	1	0.9	(2787)	1.1	(1016)	1.1	(3157)
	2	1.3	(640)	1.0	(830)	1.0	(923)
	3	1.0	(522)	0.8	(328)	0.8	(1177)
$\overline{LE}$ (W m^{-2})		72.5	(3949)	100.0	(2174)	116.6	(5257)
Sensible heat ($H/\bar{H}$)	1	0.7	(2788)	0.9	(1319)	0.6	(3157)
	2	1.8	(640)	1.3	(831)	1.6	(923)
	3	1.3	(530)	0.8	(483)	1.5	(1177)
$\bar{H}$ (W m^{-2})		9.0	(3958)	10.7	(2633)	9.4	(5257)

TABLE 3. Mean vertical gradients.

	Category	Phase I	Phase II	Phase III
Speed (m s^{-1})	1	3.8	5.6	6.0
	2	5.7	5.5	5.8
	3	4.6	4.1	4.5
ΔQ (g kg^{-1})	1	4.7	5.1	5.7
	2	4.6	4.8	5.1
	3	4.2	5.3	5.5
ΔT (°C)	1	1.1	1.1	0.7
	2	1.8	1.6	1.7
	3	1.7	1.4	2.0

The means of the three categories for each phase do not actually represent phase means, since the sample sizes are considerably smaller than the 9600 samples possible for each phase because instrument problems and the missing time periods between categories excluded data. The low number of samples in Phase II partly results from the *Oceanographer* being off station for nearly four days. The mean fluxes for each phase, although considerably different from each other, show consistency with the phase mean fluxes based on the full data set for the *Oceanographer* as well as averages for other ships (Seguin and Kidwell, 1979). The large differences in the mean fluxes between the Phase I mean values and the means in the other phases are likely due to the fact that the mean position of the Intertropical Convergence Zone (ITCZ) was south of the *Oceanographer* in Phase I, but north in Phases II and III (Martin, 1975; Hudlow, 1977; Seguin *et al.*, 1978). Therefore, the Phase I winds (and perhaps, the mean boundary-layer dynamics) and hence the fluxes behave differently than those in the other phases. Thus, we confine further discussion of the fluxes to Phases II and III.

The momentum flux, or stress (Table 2), is relatively strong in undisturbed conditions and during the density current (categories 1 and 2), and relatively small in the wake conditions (category 3). The largest contrasts occur between the wake (category 3) and the other two means. The mean wind speeds for each category (Table 3) also make this contrast evident.

The latent heat fluxes show a consistent behavior

TABLE 4. Profile summary.

Category	Number of profiles	Independent events
1 Undisturbed	55	12
2 Density current	44	21
3 Wake	20	5

with relatively large fluxes during undisturbed conditions and relatively small values during the wake. We see that no strong systematic differences exist in the moisture gradient (Table 3) in each category and that, therefore, the winds mainly govern the latent heat flux.

The sensible heat flux shows a different behavior. The largest relative values of sensible heat flux occur with the density current and again result from the relatively large wind speeds compared to the wake and relatively large temperature gradients with respect to the undisturbed case (Table 3). The sensible heat fluxes behave differently in the wake during Phases II and III. In Phase III, the large air-sea temperature differences in the wake compensate for lower wind speeds to produce relatively large sensible heat fluxes. In Phase II the air-sea temperature difference does not compensate for the reduced wind speed in the wake. The sensible heat fluxes vary as the winds and the gradients, as contrasted to the latent heat flux whose changes occur mainly because of changes in the wind. Seguin and Kidwell (1979), using data averaged over the entire observational array, also find that the sensible heat flux has variations that respond to variations in both the wind and the gradients, while the latent heat fluxes change mainly in response to changes in the winds. This implies that, while sea-air temperature gradients increase as a result of convective activity, there is no evidence of systematic variations in the low-level moisture gradients in response to convective activity. Thus, the convective overturning may bring cool air but not measurably drier air near the surface in this analysis.

The discussion above provides a qualitative description of the flux behavior as we go from undisturbed to wake conditions. The standard deviations of these mean heat fluxes amount to 30% or more of the mean in some cases. However, the differences between the disturbed categories 2 and 3 and category 1 appear significant. Because we have assumed the similarity between events within each category in Table 2, we have purposely avoided the problem of identifying "independent" events. This makes it difficult to quantify the significance of the differences between category means in Table 2.

b. Profiles

We averaged profiles of potential temperature and specific humidity for each of the three categories. We are limited to forming averages with Phase III profiles only because of the small number of independent events in each category, especially the wake, during the other phases. We use the term "independent" in the same way as we indicate the number of individual disturbances in Table 1. Often, more than one profile existed within a single event. Table 4 presents the number of profiles in each average and the number of independent events associated with each sounding. Because of the small samples of profiles in comparison to the very large samples of surface fluxes, we felt the information on the independent samples is helpful. The standard deviations of potential temperature and specific humidity are 1.0°C and 0.5 g kg^{-1}, respectively.

The mean potential temperature profiles (Fig. 3) show a distinct cooling of almost 2 K between the undisturbed conditions and the wake in the lower part of the atmosphere; above 600 m the difference between the potential temperature profiles is not great. A distinct change in slope of the mean undisturbed potential temperature profile takes place above 600 m, indicating the average top of the mixed layer. The potential temperature profile associated with category 2, the density current, shows significant low-level cooling. The lack of a distinct change in slope above 100 m of this profile indicates that the mixed layer does not exist in the density current consistent with the models of Moncrieff and Miller (1976), Betts (1976) and Zipser (1977), who all indicate that the mixed layer becomes "stripped away" during the density current. Profile data do not exist during the vigorous "squall fronts", because the BLIS did not function properly during heavy precipitation. If profiles were available for the strong squall-front cases, we would expect even greater cooling in category 2. The potential temperature profiles for the wake indicate a shallow, well-mixed layer to approximately 250 m,

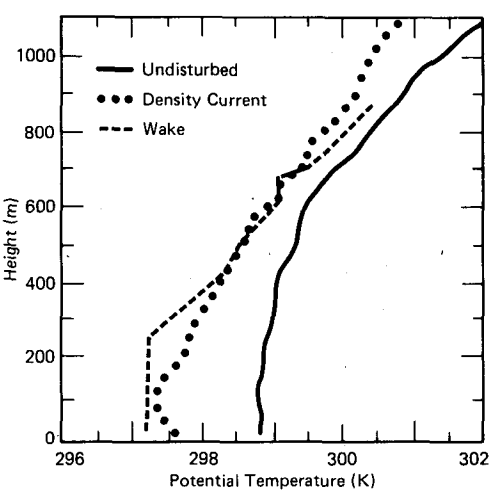

FIG. 3. Potential temperature profiles for each category.

with the upper portion of the profile warming to pre-onset temperatures.

The mean specific humidity profiles for each category show no strong systematic differences between them (Fig. 4). These results appear consistent with the observed lack of systematic changes in the moisture gradients (Table 3) near the surface and with the conceptual model presented by Zipser (1977).

5. Boundary-layer dynamics

We have the well-documented observation (Wylie, 1976; Gaynor and Mandics, 1978) that the depth of the mixed layer remains more or less constant for several hours following squall line passages, i.e., the period we have been calling the wake. During undisturbed conditions (those not influenced by a precipitating convection), we also have a case in which the depth of the mixed layer remains essentially constant. We can approximate the vertical motion due to entrainment and infer a subsidence in the more persistent wake cases (more than 4 h duration).

Deardorff (1974a) and Tennekes (1973) estimate the vertical motion due to entrainment from

$$W_e = \frac{(\overline{\theta_v' w'})_T}{\Delta\theta_v} = -A\,\frac{(\overline{\theta_v' w'})_{\text{sfc}}}{\Delta\theta_v}, \qquad (1)$$

where $(\overline{\theta_v' w'})_T$ is the buoyancy flux at the top of the mixed layer. Stull (1976a,b) indicates that other processes effect the entrainment. These include mixing due to wind shear and breaking waves, along with gravity waves with a vertical component of group velocity. Although these processes may be important, we must ignore them here because we have no way of obtaining their adequate estimation. We use the following relation to estimate $(\overline{\theta_v' w'})_{\text{sfc}}$ from the sensible and latent heat fluxes (Table 2):

$$\overline{w'\theta_v'} = (H/\rho c_p)(1 + 0.61q) + 0.61\theta E/(\rho_w), \qquad (2)$$

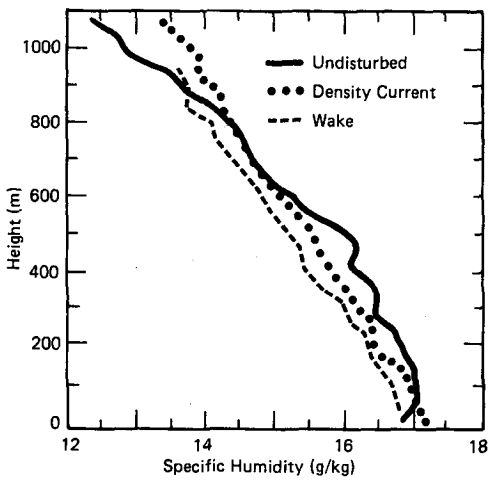

FIG. 4. Specific humidity profiles for each category.

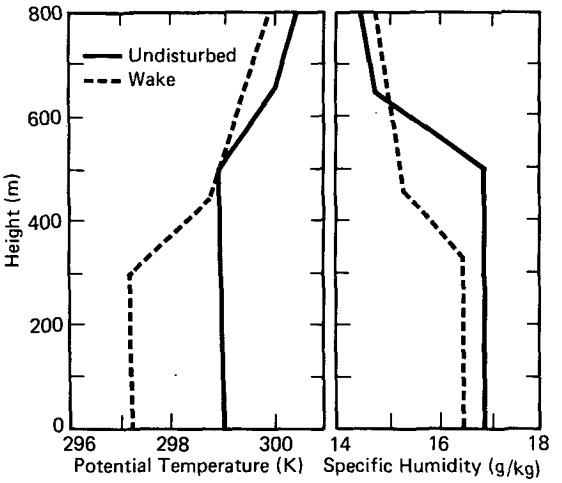

FIG. 5. Idealized profiles for undisturbed and wake conditions.

where q represents the specific humidity and the constants have their usual meanings.

Profiles of potential temperature and moisture provide estimates of the inversion strengths $\Delta\theta_v$. To calculate the inversion strength in the undisturbed and wake conditions, we first fit the individual profiles with three-line segments in a least-squares sense. The least-squares fits provide an objectively derived estimate for the inversion strengths through a smoothed or idealized set of profiles (Fig. 5). We then made composites of the idealized profiles in categories 1 and 3 to obtain $\Delta\theta_v$.

The free parameter A in (1) largely determines the magnitudes of the entrainment rates once the surface fluxes and inversion strengths are known. Several experimenters (e.g., Deardorff 1974b; Tennekes, 1973) have used a value of 0.2 for A. On the other hand, Stull (1976a) lists over 35 estimates of A, both measured and theoretical, from the literature that show values of this parameter ranging between -0.04 and 2.0. Thus, we present a range of A in Table 5. The table shows that the vertical motions due to entrainment associated with the wake are about half the values obtained for undisturbed conditions.

TABLE 5. Vertical motions due to entrainment and inversion strengths.

	Undisturbed		Wake	
A	(10^{-2} m s^{-1})	(m h^{-1})	(10^{-2} m s^{-1})	(m h^{-1})
0.05	2.8	100	1.2	45
0.10	5.7	200	2.5	90
0.20	11.4	400	5.0	180
0.30	17.1	600	7.5	270
Inversion strength (K) $\Delta\theta_v$	0.7		1.2	

Given the nearly constant height of the wake mixed layer, we expect, from Table 5, a mesoscale subsidence behind the storm ranging from 0.01 to 0.08 m s^{-1} which balances the entrainment. Zipser (1977) calculates values of W_e between 0.1 and 0.2 m s^{-1}. Our values are somewhat less because Zipser's case studies include only the most active squalls. Zipser studied the subsidence beneath the anvil following the squall. We feel justified in comparing our results with his because we are dealing with events of longer than 4 h duration. The inspection of all-sky camera photos indicated that every case with wake stable layers of this duration or longer was associated with an anvil cloud of nearly equal duration.

To estimate the divergence necessary to maintain the inversion at around 300 m in the wake (Fig. 5), we use the approximate relation

$$(\nabla \cdot \mathbf{V})_n = \frac{W_e}{T},$$

where T represents the thickness of the layer (300 m) and W_e the vertical motion due to entrainment from Table 5. The divergence estimated in this way ranges from 4×10^{-5} s^{-1} to 2×10^{-4} s^{-1}, again depending on the value chosen for A. These estimates compare favorably with the estimates of divergences (from 6×10^{-5} to 2×10^{-4} s^{-1}) in the wakes of strong squalls (Zipser, 1977) and calculated divergences associated with precipitation on the scale of 100 km (Jalickee and Ropelewski, 1979).

6. Summary and conclusions

Using the acoustic sounder facsimile record as a guide we have made composites of surface and profile data in three categories corresponding to three different atmospheric states: undisturbed, density current and wake. The latent heat fluxes and stress behave similarly during Phases II and III; in Phase I the relation of the fluxes in the various categories appears different because of the relatively low wind speeds in the undisturbed case. The density current appears well delineated by the increased sensible heat flux.

In the composites, the undisturbed mixed layer is relatively deep (500–600 m) with relatively large vertical motion due to entrainment (W_e in Table 5), while a shallow mixed layer and much smaller W_e characterize the wake. The smaller W_e values in the wake are caused by the small buoyancy fluxes calculated from Eq. (2). The implied mesoscale subsidence balancing the entrainment in the wake and maintaining a constant mixed-layer depth is smaller than the subsidence in the undisturbed boundary layer, but in reasonable agreement with Zipser (1977) who considered the more intense squall wakes. The calculated divergences agree well with other authors.

Acknowledgments. The authors appreciate the critical reviews of M. A. LeMone and E. J. Zipser. Also, we appreciate the help of J. B. Jalickee of CEAS in objectively fitting the tethered balloon profiles. At WPL, J. E. Birtwistle helped with the data reduction. The U.S. GATE Project Office supported the research.

REFERENCES

Aspliden, C. I., 1976: A classification of the structure of the tropical atmosphere and related energy fluxes. *J. Appl. Meteor.*, **15**, 692–697.

Betts, A. K., 1976: The thermodynamic transformation of the tropical subcloud layer by precipitation and downdrafts. *J. Atmos. Sci.*, **33**, 1008–1020.

Brown, E. H., and F. F. Hall, Jr., 1978: Advances in atmospheric acoustics. *Rev. Geophys. Space Phys.*, **16**, 47–110.

Burns, S. G., 1974: Boundary-layer instrumentation system. *Atmos. Tech.*, **6**, 123–128.

Charba, J., 1972: Gravity current model applied to analysis of squall-line gust front. NOAA Tech. Memo, ERL NSSL-61, National Severe Storms Laboratory, 58 pp. [NTIS COM-73-10410].

Deardorff, J. W., 1974a: Three-dimensional numerical study of the height and mean structure of a heated planetary boundary layer. *Bound.-Layer Meteor.*, **7**, 81–106.

——, 1974b: Three-dimensional numerical study of turbulence in an entraining mixed layer. *Bound.-Layer Meteor.*, **7**, 199–226.

EDS, 1975: *GATE Data Catalogue*. Environmental Data Service, NOAA, Washington, D.C.

Emmitt, G. D., 1978: Tropical cumulus interaction with and modification of the subcloud region. *J. Atmos. Sci.*, **35**, 1485–1502.

Garstang, M., and A. K. Betts, 1974: A review of the tropical boundary layer and cumulus convection: Structure, parameterization, and modeling. *Bull. Amer. Meteor. Soc.*, **55**, 1195–1205.

Gaynor, J. E., and P. A. Mandics, 1978: Analysis of the tropical marine boundary layer during GATE using acoustic sounder data. *Mon. Wea. Rev.*, **106**, 223–232.

Hall, F. F., Jr., W. D. Neff and T. V. Frazier, 1976: Wind shear observations in thunderstorm density currents. *Nature*, **264**, 408–411.

Houze, R. A., Jr., 1977: Structure and dynamics of a tropical squall-line system. *Mon. Wea. Rev.*, **105**, 1540–1567.

Hudlow, M. D., 1977: Precipitation climatology for the three phases of GATE. *Preprints 2nd Conf. Hydrometeorology*, Toronto, Amer. Meteor. Soc., 290–297.

Jalickee, J. B., and C. F. Ropelewski, 1979: An objective analysis of the boundary layer thermodynamic structure during GATE. *Mon. Wea. Rev.*, **107**, 68–76.

Johnson, R. H., 1976: The role of convective-scale precipitation downdrafts in cumulus and synoptic-scale interactions. *J. Atmos. Sci.*, **33**, 1890–1910.

Mandics, P. A., and E. J. Owens, 1975: Observations of the marine atmosphere using a ship-mounted acoustic sounder. *J. Appl. Meteor.*, **14**, 1110–1117.

——, and F. F. Hall, Jr., 1976: Preliminary results from the GATE acoustic echo sounder. *Bull. Amer. Meteor. Soc.*, **57**, 1142–1147.

——, ——, E. J. Owens and D. Wylie, 1975: Observations of the tropical marine atmosphere using an acoustic echo

sounder during GATE. *Preprints 16th Radar Meteorology Conf.*, Houston, Amer. Meteor. Soc., 257–259.

Martin, D. W., 1975: Characteristics of West African and Atlantic cloud cluster based on satellite data. GATE Rep. No. 14, Vol. I, ICSU/WMO, Geneva, 182–190.

Moncrieff, M. W. and M. J. Miller, 1976: The dynamics and simulation of tropical cumulonimbus and squall lines. *Quart. J. Roy. Meteor. Soc.*, **102**, 373–394.

Readings, C. I., E. Golton and K. A. Browning, 1973: Fine-scale structure and mixing within an inversion. *Bound.-Layer Meteor.*, **4**, 275–287.

Ropelewski, C. F., 1976: An evaluation of the meteorological data from the GATE boundary layer instrument system (BLIS). NOAA Tech. Memo. EDS-CEDDA-9, 24 pp. [NTIS PB-283-573].

Sequin, W. R., and K. B. Kidwell, 1979: Influence of synoptic scale disturbances on surface fluxes of momentum and latent and sensible heat. Accepted by *Deep-Sea Res.*

——, P. S. Sabol, R. Crayton, R. S. Cram, K. L. Echternacht and M. Poindexter, 1977: U.S. National Processing Center for GATE: B-scale surface meteorological and radiation system, including instrumentation, processing, and archived data. NOAA Tech. Rep. EDS 22, 94 pp. [NTIS PB-268-848].

——, R. B. Crayton, P. Sabol and J. W. Carlile, 1978: GATE convection subprogram data center: Final report on ship surface data validation. NOAA Tech. Rep. EDS 25 78 pp. [NTIS PB-279-560/AS].

Stull, R. B., 1976a: The energetics of entrainment across a density interface. *J. Atmos. Sci.*, **33**, 1260–1267.

——, 1976b: Mixed-layer depth model based on turbulent energetics. *J. Atmos. Sci.*, **33**, 1268–1278.

Tennekes, H., 1973: A model for the dynamics of the inversion above a convective boundary layer. *J. Atmos. Sci.*, **30**, 558–567.

Wesely, M. L., 1976: The combined effect of temperature and humidity fluctuations on refractive index. *J. Appl. Meteor.*, **15**, 43–49.

Wylie, D. P., 1976: Tropical observations of mixed layer changes caused by cumulus downdrafts taken in the GATE program. Ph.D. thesis, University of Wisconsin, 93 pp.

Zipser, E. J., 1977: Mesoscale and convective-scale downdrafts as distinct components of squall-line structure. *Mon. Wea. Rev.*, **105**, 1568–1589.